

MEASUREMENTS OF EJECTA VELOCITY DISTRIBUTION BY A HIGH-SPEED VIDEO CAMERA.

S. Yamamoto¹, N. Okabe¹, T. Kadono², S. Sugita², and T. Matsui¹, ¹Graduate School of Frontier Sciences, University of Tokyo, Chiba, Japan (yamachan@impact.k.u-tokyo.ac.jp). ²IFREE, JAMSTEC, Kanagawa, Japan

Introduction: The velocity distribution of impact ejecta (ejecta velocity distribution) from granular targets has been investigated in the laboratory for nearly three decades [e.g.1,2,3,5,7,8]. The ejecta velocity distributions for vertical impact have been determined experimentally for ejecta with velocities $v_e < \text{a few m/s}$ [1][2]. On the other hand, there are few data on velocity distribution for ejecta with $v_e > \text{a few m/s}$ (although high velocity ejecta ($v_e > 100 \text{ m/s}$) has been measured [3]). We need more data to discuss a scaling law for ejecta velocity distribution, specially for the ejecta with v_e ranging from a few to 100 m/s.

Experiments: We measure the ejecta velocity distribution for ejecta with $v_e > \text{a few m/s}$ as follows. We first measure the relation between ejection velocity, v_e , and the distance, r , from the impact site of a projectile. Next, we measure the total mass $M(r)$ of target material ejected inside the radius r . From $M(r)$ and the relation between v_e and r , we can estimate the total mass $M(v_e)$ of ejecta with velocities higher than v_e . Finally, we define $V(>v_e) = M(r)/\rho$ as the ejecta velocity distribution, where ρ is the target bulk density.

(1) Measurements of ejection velocity v_e : Figure 1 shows our experimental configuration to measure v_e . Bullet-shaped polycarbonate projectiles with a mass of 0.49 g and a diameter of 10 mm are accelerated by a single-stage gas gun. Impact velocities v_i range from 70 to 321 m/s. The impact angle to the target surface is vertical. We prepare soda-lime glass spheres with mean diameters (s) of 40 and $220 \mu\text{m}$ as the target. The glass spheres are placed in a stainless basin in a vacuum chamber with an ambient pressure $< 90 \text{ Pa}$. The targets are covered with an aluminum board with a slit (1cm width and various lengths; Fig. 1a). As shown in Fig. 1, a partition is set on the aluminum board at the distance L_1 from the impact site of a projectile. When a projectile impacts the target surface, ejecta is thrown out through the slit. Using this configuration, we can distinguish between the ejecta inside and outside the partition (Fig. 1b). A high-speed video camera allows us to measure ejection velocity v_e of ejecta outside the partition.

Figure 2 shows the scaled ejection velocity v_e/v_i against the distance $r = (L_1 + L_2)/2$. It is clear that the scaled ejection velocity decreases exponentially as r increases. Assuming a power-law relation between v_e/v_i and r , the slopes (dashed lines in Fig.2) for targets $s=40$ and

$220 \mu\text{m}$ are estimated to be -2.02 and -2.01 , respectively. Figure 2 shows that the power-law relations for $s=40$ and $220 \mu\text{m}$ are quite similar, indicating that the scaled ejection velocity does not depend on target grain size.

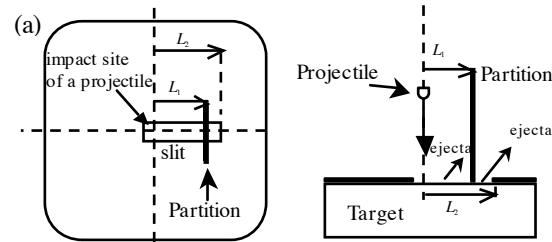


Figure 1: Schematic figure of the experiments to measure the ejection velocity v_e (top view (a) and side view (b)).

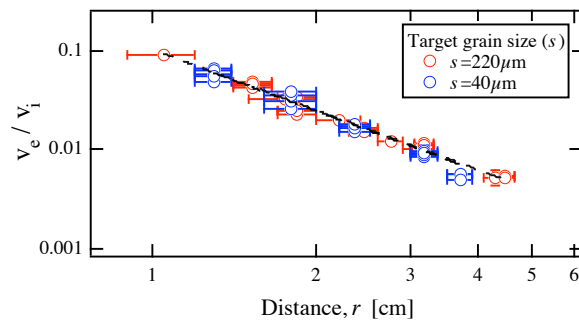


Figure 2: The scaled ejection velocity (v_e/v_i) is plotted against distance (r). Dashed lines indicate the best-fit curves for $s=40$ and $220 \mu\text{m}$, respectively.

(2) Measurements of $M(r)$: We next measure the total mass $M(r)$ of target material ejected inside the radius r as follows: the stainless basin with the glass sphere target is covered by an aluminum board with a centered hole of a radius r . When a projectile impacts at the center, ejecta are thrown out through the hole. After each experiment, we collect the ejecta that were thrown out through the hole and measure its mass. When the crater radius R is smaller than the hole radius ($R < r$), the collected ejecta mass depends on the impact velocity v_i . On the other hand, it has been shown that, when $R > r$, the collected ejecta mass is independent of v_i [4]. In this study, $M(r)$ is defined as the ejecta mass collected when $R > r$. Figure 3 shows $M(r)$ vs. r , and we see that $M(r)$ increases exponentially with increasing r . Assuming a power-law relation between $M(r)$ and r , the least-square fit for $s=40$ and $220 \mu\text{m}$ gives $M(r) = 0.70r^{3.00}$ and $M(r) = 0.84r^{3.15}$, respectively (dashed lines in Fig. 3). Thus $M(r)$ is nearly proportional to the cube of r . We can see in Fig. 3 that

$M(r)$ for $s=220\mu\text{m}$ is slightly greater than that for $s=40\mu\text{m}$. This may suggest that the volume (and depth) of the excavation region in impact cratering depends on the target grain size.

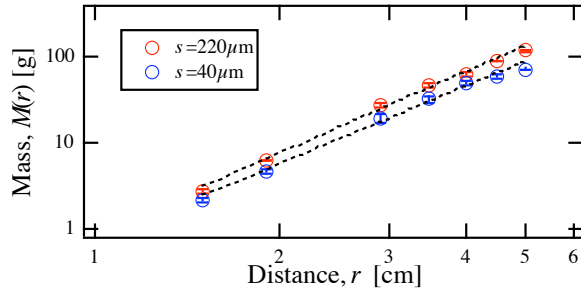


Figure 3: Mass of material ejected inside the radius r . Dashed lines indicate the best-fit curves for $s=40$ and $220\mu\text{m}$, respectively.

Results and discussion: From the v_e and $M(r)$ obtained, we estimate the ejecta velocity distribution $V(>v_e) = M(r)/\rho$, where the target bulk density ρ for $s=40$ and $220\mu\text{m}$ are measured to be 1.50 and 1.59g/cm^3 , respectively. In Figure 4, we plot $V(>v_e)$ against the scaled ejection velocity v_e/v_i . It is clear that $V(>v_e)$ decreases exponentially with increasing v_e/v_i . Assuming a power-law relation between $V(>v_e)$ and v_e/v_i , the least-square fit (dashed lines) for $s=40$ and $220\mu\text{m}$ gives $V(>v_e)=0.013v_e^{-1.58}$ and $V(>v_e)=0.017v_e^{-1.43}$, respectively. It is not clear whether $V(>v_e)$ depends on target grain size, although $V(>v_e)$ for $s=40\mu\text{m}$ seems to be less than that for $s=220\mu\text{m}$.

Our current results are plotted on the non-dimensional $\Pi_{\text{vol}}-\Pi_{\text{ev}}$ diagram in Fig. 5, where $\Pi_{\text{vol}}(=V(>v_e)/R^3)$ is nondimensional ejecta volume and $\Pi_{\text{ev}}(=v_e/(gR)^{0.5})$ is nondimensional ejection velocity (R is crater radius and g is gravitational acceleration)[1]. It is clear in this figure that Π_{vol} for $s=40$ and $220\mu\text{m}$ decreases exponentially with increasing Π_{ev} . Assuming a power-law relation between Π_{vol} and Π_{ev} , the least-square fit for $s=40$ and $220\mu\text{m}$ gives $\Pi_{\text{vol}}=0.18\Pi_{\text{ev}}^{-1.41}$ and $\Pi_{\text{vol}}=0.18\Pi_{\text{ev}}^{-1.54}$, respectively. Our results may suggest that the power-law exponent in the $\Pi_{\text{vol}}-\Pi_{\text{ev}}$ relation for granular targets depends on the target grain size.

In previous studies, the power-law relation ($\Pi_{\text{vol}}=0.32\Pi_{\text{ev}}^{-1.22}$)[1] based on explosion experiments ($v_e<\sim 10\text{m/s}$) has been suggested as the scaling law for the ejecta velocity distribution. For a comparison, this relation is also plotted in Fig. 5 (green dotted line). We can see that the present results for $s=40$ and $220\mu\text{m}$ deviate from the power-law relation. This difference increases with increase in Π_{ev} . In addition, other experimental data on the impact ejecta with $v_e<\sim 2\text{ m/s}$

(Stöffler et al. [5]; their target is quartz sand) are also plotted (open triangle) in Fig. 5. We can see in this figure that the data by Stöffler et al. are slightly greater than the present results for $\Pi_{\text{ev}} < 2$.

Figure 5 shows that the present results are not consistent with previous scaling law and other data. This might be explained as follows. For the nondimensional parameters Π_{vol} and Π_{ev} , $V(>v_e)$ and v_e are scaled by the crater radius R . However, it has been shown that R depends on target material and the grain size [e.g. 4, 6]. Thus the scaling with R may lead to the difference in Π_{vol} and Π_{ev} between these data in Fig. 5.

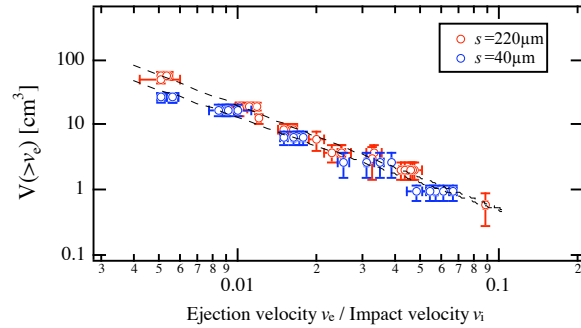


Figure 4: Volume $V(>v_e)$ of ejecta with velocity higher than v_e is plotted against v_e/v_i for $s=40$ and $220\mu\text{m}$. Dashed lines indicate the best-fit curves for $s=40$ and $220\mu\text{m}$, respectively.

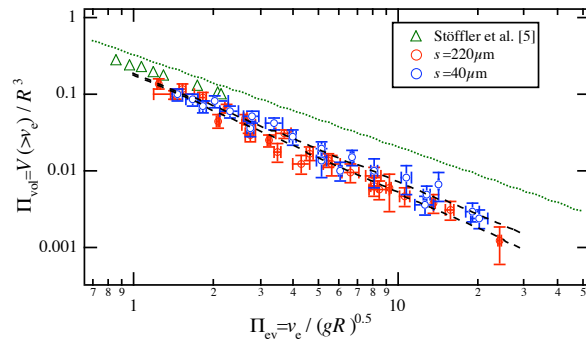


Figure 5: The nondimensional ejecta volume Π_{vol} is plotted against the nondimensional ejecta velocity Π_{ev} for the present results. For comparison, a scaling formula (dotted line) [1] and the data on the low velocity ejecta by Stöffler et al. [5] are also plotted.

References: [1] Housen K.R. *et al.*, (1983) *JGR*, 88, 2485-2499. [2] Hartmann W.K., (1985) *Icarus*, 63, 69-98. [3] Yamamoto S., *et al.*, (2004) submitted to *Icarus*. [4] Yamamoto et al. (2004), 35th LPSC, #1482. [5] Stöffler *et al.* (1975) *JGR*, 80, 4062-4077. [6] Schmidt R.M., 1980, *Proc. LPSC* 11th, 2099-2128. [7] Yamamoto S., (2002) *Icarus*, 158, 87-97. [8] Yamamoto S. & Nakamura A.M., (1997) *Icarus*, 128, 160-170.